Lower Acicular Ferrite

A.A.B. SUGDEN and H.K.D.H. BHADESHIA

An experiment has been designed to confirm that the mechanism of growth of acicular ferrite in steel welds is similar to that of bainite in ordinary steels. On the hypothesis that the growth mechanisms are identical, it was expected that if the carbon concentration of a weld is increased sufficiently, then for similar welding conditions, the microstructure should undergo a transition from acicular ferrite to *lower* acicular ferrite, in which the plates of acicular ferrite should contain cementite particles of the sort normally associated with lower bainite in wrought steels. An experimental weld of unusually high carbon concentration was prepared, and metallography confirmed the existence of lower acicular ferrite, supporting the conclusion that acicular ferrite is simply an intragranularly nucleated bainite.

I. INTRODUCTION

THERE is general agreement[1–4] that a weld microstructure containing mainly acicular ferrite will exhibit high strength and optimum toughness due to its small "grain size" and the way in which the plates of ferrite are dispersed in the microstructure, causing the plane of a cleavage crack to be frequently deflected. In contrast, the presence of allotriomorphic ferrite, parallel formations of Widmanstätten ferrite plates, or grain-boundary nucleated sheaves of bainite is considered to be detrimental to the toughness of the weld, because these constituents allow cracks to propagate without much deflection. The problem is, in fact, more complicated, since it appears that there are instances when large amounts of acicular ferrite do not lead to the best toughness.[5] Whatever the optimum microstructure, it is clear that a better understanding of the phases involved would permit more detailed investigation of the relationship with mechanical properties. In this context, acicular ferrite is the least understood of all the main phases that occur in steel welds.

The nature of the acicular ferrite phase has been the cause of much research. In fact, the term "acicular ferrite" is a misnomer. In two dimensions, acicular ferrite appears as "randomly" oriented, needle-shaped particles, but this belies its true morphology, which is that of a thin, lenticular plate. For a typical low-alloy C-Mn steel weldment, acicular ferrite will begin to appear during cooling in the range of 500 °C to 440 °C,[6] a temperature range which is consistent with the observation of plate morphologies of ferrite in wrought steels.

It is well established that acicular ferrite nucleates at nonmetallic inclusions which occur frequently in arc-weld deposits, but its mechanism of growth has not been clear. Its appearance alone has sometimes led to proposals that it is Widmanstätten ferrite.[7,8,9] However, few investigations have focused on the details of the transformation mechanism. There is some evidence that the formation of acicular ferrite causes an invariant plane strain shape deformation of the transformed region.[10,11] The acicular ferrite *always* has an orientation relationship with the austenite grain in which it grows, such that one of its closest packed {110} planes is nearly parallel to a close-packed {111} plane of the parent austenite; within these planes, a close-packed $\langle 11\bar{1} \rangle$ direction of the acicular ferrite is found to be near a close-packed $\langle \bar{1}01 \rangle$ direction of the austenite.[10] These considerations indicate that the growth of acicular ferrite occurs by displacive transformation, and the strain energy due to the accompanying shape deformation is a major contribution to the ~400 $Jmol^{-1}$ of stored energy associated with the acicular ferrite transformation.[10,12,13] The fact that plates of acicular ferrite are never found to grow across austenite grain boundaries is consistent with the displacive transformation mechanism, since the necessary coordinated movements cannot, in general, be sustained across austenite grain boundaries.[10]

With respect to the carbon concentration of acicular ferrite during transformation, experiments and thermodynamic theory have demonstrated that the growth of acicular ferrite is diffusionless,[10–13] the ferrite inheriting the chemical composition of the parent austenite. However, immediately after transformation, the excess carbon in the acicular ferrite is rejected into the residual austenite. This latter process can occur in a matter of seconds.[14,15] As a consequence, the acicular ferrite transformation obeys an "incomplete reaction phenomenon"[14,15,16] in which the amount of acicular ferrite that forms at any given transformation temperature is less than required by equilibrium, the reaction stopping when the carbon concentration of the residual austenite reaches the T_o' curve of the equilibrium or paraequilibrium phase diagram (for plain carbon or alloy steels, respectively), where austenite and acicular ferrite of the same composition have equal free energies.

All of the characteristics of acicular ferrite discussed here indicate that it is essentially identical to bainite.[14,15] It differs morphologically from the bainite found in wrought steels, because it nucleates intragranularly on inclusions and, in low-alloy steel weld deposits, is unable to adopt a sheaf morphology because of physical impingement with other plates nucleated nearby. It has been demonstrated that an acicular ferrite morphology is favored when the density of intragranular nucleation sites is large compared with nucleation sites at austenite grain

A.A.B. SUGDEN, Research Scientist, and H.K.D.H. BHADESHIA, University Lecturer, are with the Department of Materials Science and Metallurgy, University of Cambridge, Pembroke Street, Cambridge CB2 3QZ, United Kingdom.

Manuscript submitted November 28, 1988.

surfaces.[12,13,17] In a weld deposit with a given inclusion content, when the austenite grain size is large, acicular ferrite is obtained by isothermal transformation in the bainite temperature range. For the same transformation conditions, if the austenite grain size is small, then the formation of conventional bainite sheaves from the austenite grain surfaces forestalls the development of events within the austenite grains, especially since heterogeneous nucleation at inclusions requires a higher activation energy relative to nucleation at grain surfaces.[18]

Bainite occurs in two main microstructural forms—upper and lower bainite. In upper bainite, carbide particles precipitate from the residual austenite between the platelets of bainitic ferrite, whereas in lower bainite, carbides may also precipitate from within the supersaturated bainitic ferrite. This latter precipitation usually gives rise to a single crystallographic variant of carbide, whose habit plane is inclined at an angle of ~60 deg to the habit plane of the bainitic ferrite plane.[19] The transition from upper to lower bainite can be understood in terms of the processes which occur immediately after the diffusionless growth of bainitic ferrite: the excess carbon in the ferrite can diffuse into the residual austenite or precipitate in the ferrite as carbides. If the former diffusion process dominates (as it might at relatively high temperatures), then upper bainite is obtained, whereas at lower temperatures where diffusion becomes more sluggish, the supersaturation is partly relieved by the precipitation of carbides, giving rise to classical lower bainite.

The purpose of the present work was to confirm further the analogy between acicular ferrite and bainite[10,13] by attempting to produce a "lower acicular ferrite." Conventional acicular ferrite has never been observed to contain any carbide precipitates, but this is probably because ordinary weld deposits, for reasons of toughness, contain relatively low carbon concentrations. Under suitable conditions, for example, by increasing the carbon concentration of the weld, it should be possible to observe a transition to lower acicular ferrite, which may then contain carbide precipitates within the plates of acicular ferrite in a distribution and crystallography which is characteristic of conventional lower bainite found in wrought steels.

II. EXPERIMENTAL METHOD

In order to expect to see intragranularly nucleated lower bainite, an unusual weld would have to be fabricated with a chemical composition which retards the partitioning of carbon from supersaturated ferrite and, hence, provides an opportunity for carbide precipitation to occur within the plates of acicular ferrite. Assuming that a plate of acicular ferrite forms without diffusion, the time t_d required to decarburize it to a paraequilibrium carbon concentration is given approximately by[14,15]

$$t_d^{0.5} = \frac{t_h(\bar{x} - x^{\alpha\gamma})\pi^{0.5}}{4\bar{D}^{0.5}(x^{\gamma\alpha} - \bar{x})} \qquad [1]$$

where t_h is the thickness of the ferrite plate, $x^{\gamma\alpha}$ and $x^{\alpha\gamma}$ are the paraequilibrium carbon concentrations of austenite and ferrite, respectively, calculated after allowing for the stored energy of the ferrite,[20] $\bar{D}$ is the integrated average diffusivity of carbon in austenite, and $\bar{x}$ is the average carbon concentration in the alloy concerned. $\bar{D}$ is calculated as follows:[21]

$$\bar{D} = \int_{\bar{x}}^{x^{\gamma\alpha}} \frac{D\{x,T\}dx}{(x^{\gamma\alpha} - \bar{x})} \qquad [2]$$

where $D\{x,T\}$ is the diffusivity of carbon in austenite as a function of carbon concentration and temperature, as discussed in References 22 through 24.

It is evident from Eq. [1] that an increase in the carbon concentration of the alloy should also increase the time required to decarburize the ferrite plates. Therefore, an ISO-2560 multirun manual-metal-arc weld was fabricated from 200 mm thick plate. The arc current and voltage were 180 A and 23 V, respectively, with dc positive electrode polarity and no preheat. The welding speed was approximately 4 mm/s. In accordance with the specification, the maximum interpass temperature was 250 °C. The carbon content of the weld metal was controlled using specially designed 4 mm diameter carbon-coated electrodes to give a weld metal whose composition is given in Table I. Note that the ISO-2560 joint geometry is commonly used in the study of weld metal properties, since it ensures an all-weld deposit with a minimum of dilution from the base plate, which was made of mild steel of 20 mm thickness and a chemical composition Fe-0.094C-0.21Si-0.71Mn wt pct.

A weld with a high (0.3 wt pct) carbon content was chosen as the simplest way by which lower acicular ferrite could be expected to be seen. The concentration of manganese was chosen to avoid the formation of phases such as allotriomorphic and Widmanstätten ferrite; calculations using a model[25,26] for the prediction of the microstructure of welds indicated that for the deposition conditions used, the as-deposited microstructure should consist of just acicular ferrite, martensite, and retained austenite. The silicon addition is at the usual level for manual-metal-arc weld deposits, its purpose being to act as a deoxidizing element during welding.

In the design of weld deposits containing acicular ferrite, the role of oxides and other nonmetallic inclusions is known to be important.[1–4] Although a low weld metal oxygen context could lead to the generation of bainitic microstructures by depriving the interior of the columnar austenite grains of nucleation sites for acicular ferrite, this was not desired, since the experiment aimed to isolate intragranularly nucleated, rather than grain-boundary nucleated, bainite. However, the oxygen content should not be too high either, since multiple nucleation events would lead to hard impingement between plates, masking the morphology of the product phase. In light of this, an oxygen content in the range of 100 to 200 ppm seemed intuitively desirable. It can be seen that the oxygen content obtained experimentally is within the range intended.

Electrolytic etching of the weld metal was carried out in an aqueous solution of 20 pct NaOH by volume, at a voltage of 10 volts, for 45 seconds. Thin foils for transmission electron microscopy (TEM) were prepared from 3 mm diameter discs machined from the top (unreheated) bead of the weld. The discs were ground sequentially on 400, 1200, and 4000 mesh SiC paper to a

Table I. Weld 1: Weld Metal Composition Analysis (Weight Percent)

C	Si	Mn	Cr	Ni	Mo	P	S	O	N
0.32	0.48	1.65	0.03	0.03	0.01	0.011	0.005	0.0141	0.0064

thickness of 0.05 mm and then electrochemically profiled using a twin-jet Fischione electropolisher. Polishing was carried out at a voltage of 40 V and at room temperature in an electrolyte of 5 pct perchloric acid/25 pct glycerol in ethanol.

III. RESULTS

The influence of carbon in promoting the formation of lower bainite is, in fact, far greater than implied by Eq. [1]. An increase in carbon concentration also depresses the various transformation temperatures (Figure 1(a)),[27] so that diffusion has to occur at lower temperatures and, hence, is more sluggish (*i.e.*, t_d increases). Figure 1(b) shows calculations of t_d carried out using Eq. [1] for a range of carbon concentrations and for transformation temperatures between the B_s and M_s for the steels concerned. It is clear that there is a substantial increase in the time needed to decarburize a supersaturated plate of bainite for the higher carbon steel whose composition corresponds to that of weld 1. On the other hand, for the steel with the lowest carbon concentration (0.08 wt pct), which is typical of conventional weld deposits, the decarburization is expected to occur so rapidly that it may explain the absence of any lower bainite/acicular ferrite conventional welds which are continuously cooled.

Figure 2 shows the solidification microstructure of the top bead of the weld. It has been demonstrated in other work that, because of the high cooling rates found in MMA welding, a carbon content of 0.30 wt pct or greater will be liable to induce solidification from the melt as austenite in a low-alloy steel, rather than the usual δ-ferrite.[28,29] That solidification occurred as austenite is confirmed by the strong directionality of the microstructure due to unrestricted grain growth in the liquid phase and by the fact that the cells within the grains were found to change orientation only at the columnar boundaries.

Figure 3 shows details of the microstructure with the specimen etched using nital. The cell boundaries can be seen to be delineated by a discontinuous, light-etching phase. The interior of the cells was found to be difficult to resolve using optical microscopy. Hardness testing was used to help characterize the microstructure. The hardness of the specimen (Vickers 10 kg) was found to be (with a 95 pct confidence) 299 ± 2.2 HV. Using a Zeiss microhardness tester, the dark region of the weld metal structure (*i.e.*, the microstructure within the cells) gave a hardness of 448 ± 32 HV. However, microhardness measurements of the discontinuous grain boundary phase gave a reading of 664 ± 36 HV. This indicates that although the cell boundary phase superficially resembles allotriomorphic ferrite, it is martensitic in nature. In fact, martensitic transformation at cell boundaries can be seen in high-strength weld deposits due to the large amount of solute segregation that occurs during solidification.[2] However, this does not appear to have been reported previously in low C-Mn welds. The most likely reason is that low-alloy steels usually solidify as δ-ferrite when the resultant alloying element segregation is not so great. In this work, however, solidification occurred as primary austenite, which characteristically results in a much larger amount of chemical microsegregation, making martensite formation at the cell boundaries more likely.

It will be noted that the microhardness readings of the individual phases are both higher than the macrohardness value reported for the weld as a whole. This occurs as a consequence of the so-called "indentation size effect." It is a recognized phenomenon that the hardness

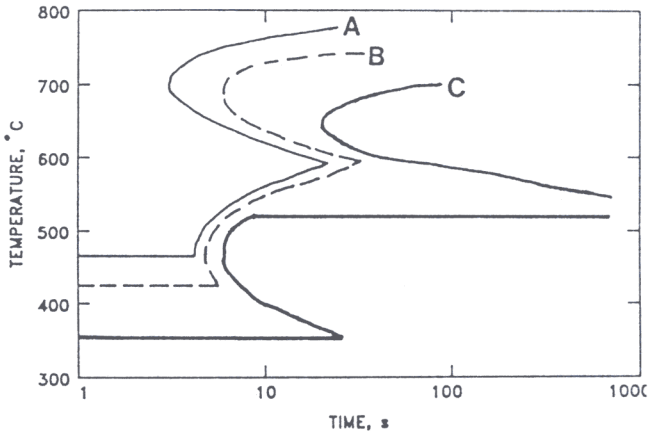

(*a*)

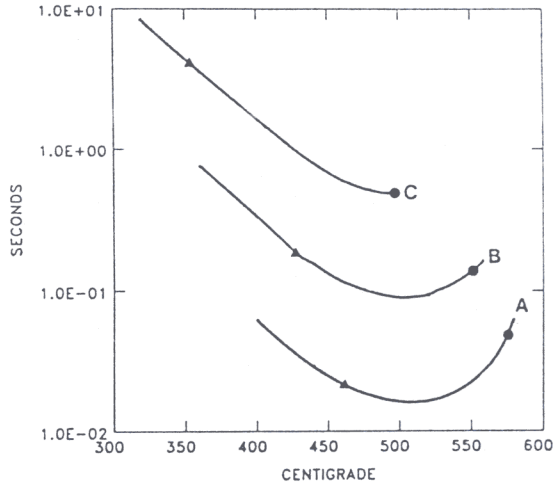

(*b*)

Fig. 1—(*a*) Isothermal TTT diagrams for a steel with the same composition as weld 1 (C), and for two similar steels (A and B) with reduced carbon concentrations of 0.08 and 0.16 wt pct C, respectively. Calculated using the method described in Ref. 27. (*b*) Plots of the time required to decarburize a plate of ferrite of thickness 0.5 μm to its equilibrium carbon concentration, as a function of temperature and the mean carbon concentration of the alloy. Steel C has the same composition as weld 1, whereas steels A and B differ only in their lower carbon concentrations of 0.08 and 0.16 wt pct C, respectively. The points represent the calculated bainite-start (dots) and martensite-start temperatures (triangles).

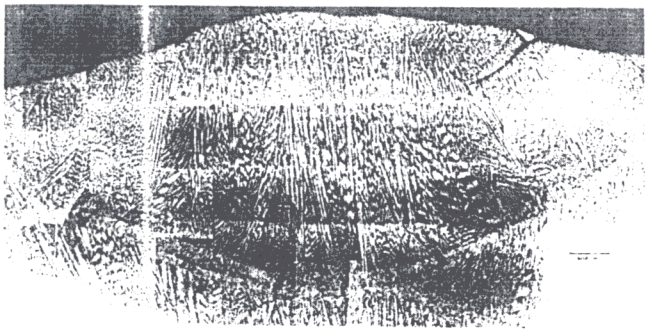

Fig. 2—Weld metal microstructure (top bead) showing solidification structure lightly electrolytically etched in saturated aqueous sodium hydroxide, followed by an etch using 2 pct nital.

of a material increases with decreasing load.[30] The microhardness measurements in our work had to be made using the smallest available load to ensure that the indent size was much less than the dimensions of the cell boundary phase. The applied load was, therefore, only 1/1000th the macroload of 10 kg, and this caused the observed microhardness to increase. However, the comparison made between the hardnesses of the two phases recorded for the same applied load is still quite valid.

The weld proved difficult to etch, probably because of its unusual composition and, as will be seen later, profuse cementite precipitation. However, the microstructure of the weld was successfully revealed by electrolytic etching in saturated aqueous sodium hydroxide (Figures 4(a) and (b)) and a dilute preparation of nital, when the weld was found to contain a large amount of fine-grained acicular ferrite. Inclusions can also be seen in Figure 4(a), located at the cell boundaries, thus confirming earlier work on the nonuniform distribution of inclusions in steel weld deposits,[28] where it was demonstrated that during solidification, larger inclusions tend to be located at the cusps in the solid/liquid interface, thereby becoming trapped at the cell boundaries in the resulting solid phase.

Transmission electron micrographs from samples prepared from the top bead of the weld are given in Figures 5 through 11. The microstructure of the weld metal in the vicinity of the prior-austenite grain boundaries consisted predominantly of grain-boundary nucleated upper bainite, as shown in Figures 5(a) and (b). Allotriomorphic ferrite formation was inhibited by the generally high alloy concentration of the weld and because solidification proceeded with austenite as the primary phase.*

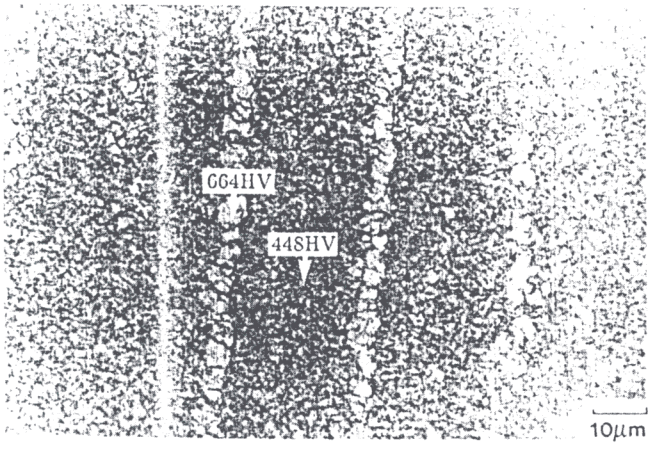

Fig. 3—Microstructure of the as-deposited weld metal. Vickers (10 g) hardness are indicated for cell boundaries and for the weld metal microstructure between them. Etchant: 2 pct nital.

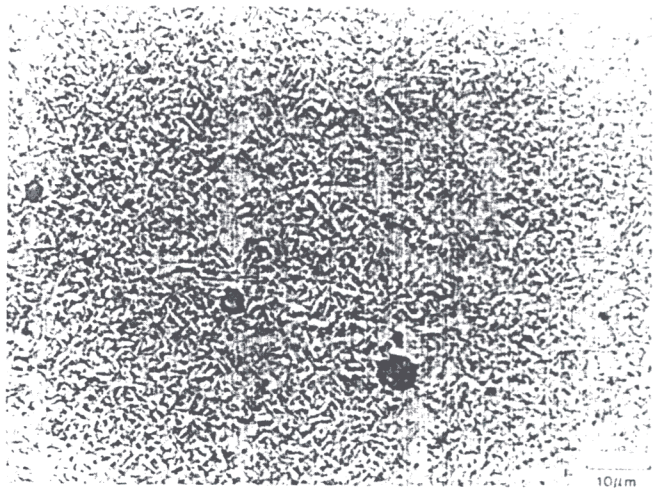

(*a*)

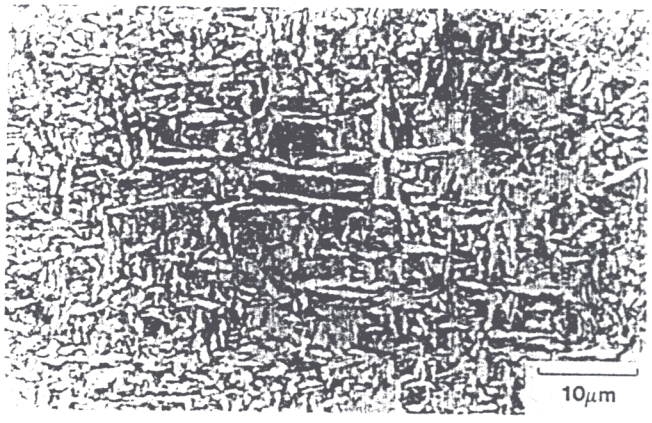

(*b*)

Fig. 4—Weld 1: details of the as-welded microstructure (*a*) electrolytically etched in saturated aqueous sodium hydroxide and (*b*) etched in 0.5 pct nital.

*When solidification at nonequilibrium cooling rates occurs with austenite as the primary phase, the segregation during solidification leads to solute-rich regions which are expected to coincide with the austenite grain boundaries. Since these are the regions where allotriomorphic ferrite nucleates, its formation kinetics will be retarded. On the other hand, when solidification proceeds with δ-ferrite as the primary phase, the subsequent formation of austenite occurs in such a way that the original δ-δ grain boundaries (which are in the solute-rich regions) do not, in general, coincide with the austenite grain boundaries.

This led to a microstructure at the austenite grain boundaries which was found to be completely different from that normally encountered in low-carbon C-Mn weld deposits where allotriomorphic ferrite and Widmanstätten ferrite are present in significant proportions.

The usual platelets of acicular ferrite, which are an

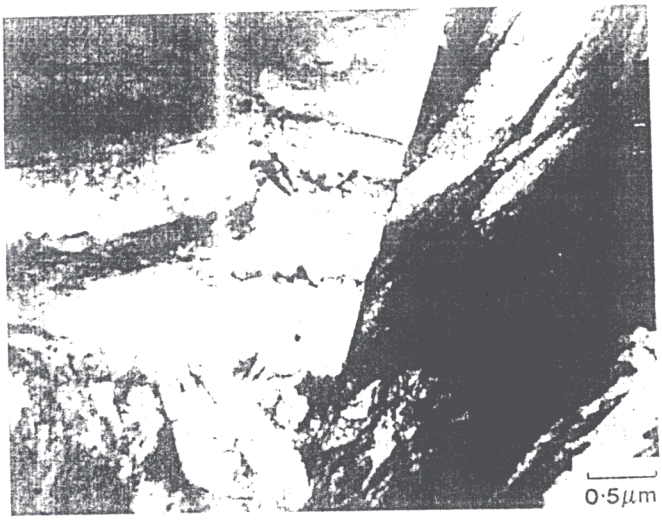

(*a*)

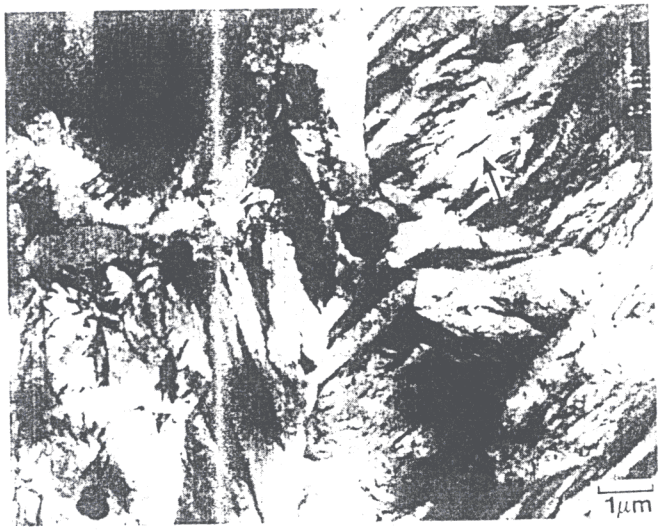

(*b*)

Fig. 5—Classical bainite subunits nucleated as the austenite grain boundaries of weld 1. The gray phase between the subunits in (*a*) is likely to be retained austenite. Lower bainitic carbides (arrowed) may be seen within the ferrite toward the top right of (*b*).

instantly recognizable feature of low-carbon weld deposits, were found to be present within the columnar austenite grains; these correspond to intragranularly nucleated bainite (Figure 6). Other platelets appear to have nucleated around those which initially nucleated at inclusions, rather like the autocatalytic nucleation associated with the formation of sheaves of bainite.

In addition to the conventional acicular ferrite platelets, spectacular formations of intragranularly nucleated "lower acicular ferrite" plates were also observed (Figures 7 through 9). These were, in all respects, identical to conventional acicular ferrite, except that each plate contained a single orientation variant of cementite precipitates whose habit planes were inclined to the apparent plate axis. The cementite particles were found to exhibit a Bagaryatski orientation relationship with the ferrite in which they precipitated (Figure 10). The microstructure of the lower acicular ferrite plates was found to be ex-

Fig. 6—Microstructure of weld metal within the columnar grains showing long platelets of acicular ferrite, some of which seem to originate at inclusions. There is also evidence for the subsequent autocatalytic formation of other platelets (arrowed) on the platelets which formed first by heterogeneous nucleation at inclusions.

actly identical to that of lower bainite found in wrought steels, except that the clusters of plates nucleated at inclusions are not in the form of well-developed sheaves. The fact that a mixed microstructure of carbide-free acicular ferrite (*i.e.*, intragranularly nucleated upper bainite) and lower acicular ferrite (*i.e.*, intragranularly nucleated lower bainite) was observed is probably a reflection of the fact that the microstructure formed by continuous cooling transformation (Figures 7 and 11).

The growth of lower bainite in a weld in the manner of intragranularly nucleated plates has previously been unseen. The development of this unusual microstructure may be interpreted as being a consequence of the relatively high amount of carbon present in the weld, as in

Fig. 7—Weld metal microstructure showing nonparallel platelets of lower acicular ferrite containing cementite particles. The residual regions between the platelets contain mainly martensite.

Fig. 8—Photomontage of the microstructure of weld 1 within the columnar grains showing a lower bainite-type microstructure in a region where the degree of transformation is relatively large.

general, a high carbon concentration will lead to an increased likelihood of lower bainite formation. This is apparent from Figure 1, which shows a calculated isothermal time-temperature-transformation (TTT) diagram and a diagram illustrating the time taken to decarburize a plate of carbon-supersaturated ferrite for a steel with the same composition as weld 1, and compares this with TTT curves calculated for steels with one-half and one-quarter the carbon concentrations of the weld metal. The effect of the high carbon concentration is to provide a longer time period for the precipitation of carbides within the ferrite and, thus, give a transition from upper to lower bainite/acicular ferrite.

Given that acicular ferrite seems to have all the characteristics of bainite, except that it nucleates intragranularly and heterogeneously at inclusions, it is natural to expect an "upper" and "lower" morphology of acicular ferrite. Since it is necessary to distinguish between the two bainitic phases observed, it is, therefore, proposed that they should be referred to as upper acicular ferrite and lower acicular ferrite. However, since lower acicular ferrite is most unlikely to be found in ordinary welds, which, for reasons of toughness, contain very little carbon, it is emphasized that the importance of the present results is really to throw light on the mechanism of the acicular ferrite transformation, rather than to propose any new classification scheme.

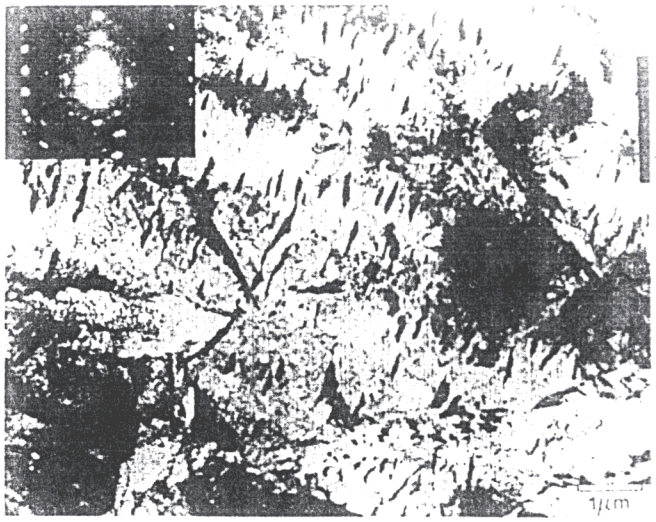

(*a*)

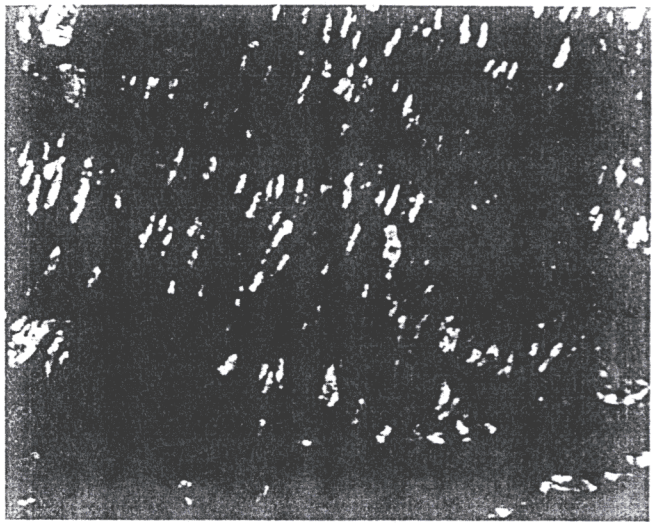

(*b*)

Fig. 9—(*a*) Bright-field image of weld metal microstructure and (*b*) dark-field image taken using a $(0\bar{1}3)$ cementite reflection.

IV. SUMMARY

The microstructure of an ISO-2560 geometry manual-metal-arc weld deposit of composition Fe-0.32C-1.65Mn-0.48Si (wt pct) was examined optically and using TEM. The as-welded microstructure was found to consist of columnar austenite grains which formed directly from the liquid phase. Microhardness measurements demonstrated that the regions in the vicinity of the solidification-cell boundaries of the weld metal microstructure were largely martensitic, probably due to their enrichment with hardenability enhancing solutes during solidification. Transmission electron microscopy revealed that the microstructure within the austenite grains consisted of a mixture of acicular ferrite, bainite, and martensite. The bainite was in the form of classical sheaves nucleated at the austenite grain boundaries, whereas the acicular ferrite consisted of the "interlocking" plates of ferrite of the kind normally associated with steel weld deposits.

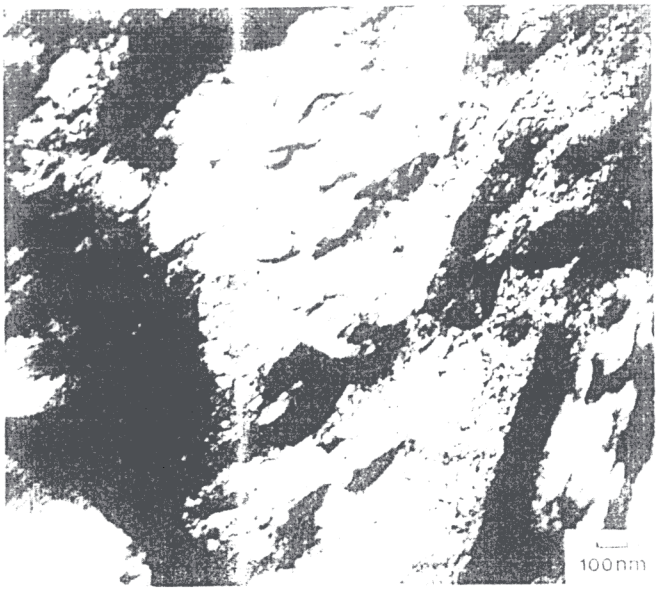

(*a*)

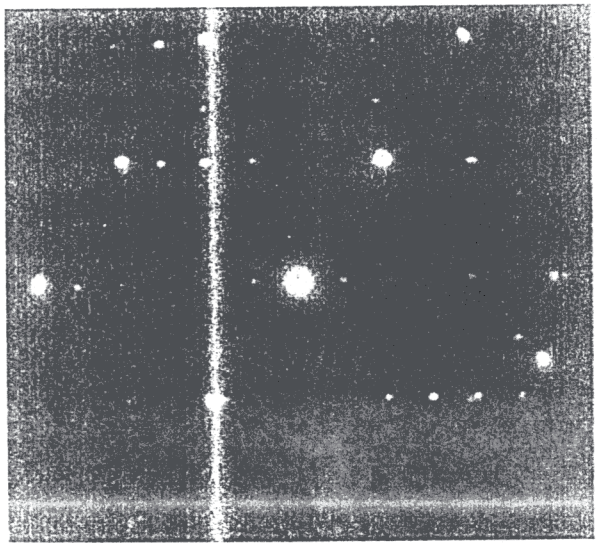

(*b*)

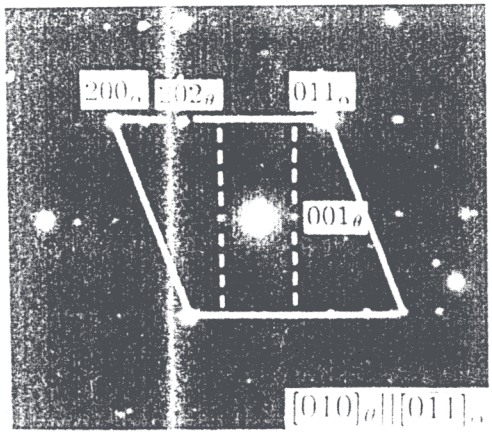

(*c*)

Fig. 10—(*a*) High magnification micrograph showing carbides inside the ferrite plates, (*b*) diffraction pattern, and (*c*) interpretation of diffraction pattern. The carbides exhibit a Bagaryatski orientation relationship with the ferrite matrix.

Fig. 11—Micrograph of weld 1 showing an oxide inclusion surrounded by acicular ferrite plates. Both upper and lower acicular ferrite can be seen.

However, some of these acicular ferrite plates were found to contain arrays of cementite precipitates, the particles within a given plate being of the same crystallographic variant of the Bagaryatski orientation relationship. These plates are designated "lower acicular ferrite" by analogy with lower bainite found in wrought steels; the carbide precipitation observed in the lower acicular ferrite plates was, in all respects, found to be identical to that observed in conventional lower bainite. The observation of the unusual microstructure of lower acicular ferrite can be rationalized qualitatively in terms of a model for the transition from upper to lower bainite, in which the transition is predicted, when the time required for carbon to diffuse out of a supersaturated plate of ferrite is sufficiently high to permit the precipitation of carbides within the ferrite.

The results confirm the conclusions of other work that the mechanism of acicular ferrite formation is, in essence, identical to that of bainite, except that the morphology of acicular ferrite differs, since it nucleates intragranularly from point sites, and physical impingement between plates nucleated from adjacent inclusions prevents the full development of the sheaf morphology associated with conventional bainite.

ACKNOWLEDGMENTS

The authors are grateful to the Science and Engineering Research Council and to ESAB AB (Sweden) for financial support and to Professor D. Hull for the provision of laboratory facilities at the University of Cambridge. The authors are grateful for the technical assistance provided by S. Atamert and Professor J.-R. Yang.

REFERENCES

1. R.J. Pargeter: *Weld. Inst. Res. Bull.*, 1983, vol. 7, pp. 215-20.
2. O. Grong and D.R. Matlock: *Int. Met. Rev.*, 1986, vol. 31, pp. 27-48.
3. D.J. Abson and R.J. Pargeter: *Int. Met. Rev.*, 1986, vol. 31, pp. 141-94.

4. R.A. Farrar and P.L. Harrison: *J. Mater. Sci.*, 1987, vol. 22, pp. 3812-20.
5. E.S. Kayali, A.J. Pacey, and H.W. Kerr: *Can. Metall. Q.*, 1984, vol. 23 (2), pp. 227-36.
6. Y. Ito and M. Nakanishi: *Sumitomo Search*, 1982, no. 15, p. 42.
7. D.J. Abson, R.E. Dolby, and P.H.M. Hart: in *Trends in Steels and Consumables for Welding*, Proc. Conf., Welding Institute, Abington, U.K., 1978, pp. 75-101.
8. R.C. Cochrane and P.R. Kirkwood: in *Trends in Steels and Consumables for Welding*, Proc. Conf., Welding Institute, Abington, U.K., 1978, pp. 103-21.
9. D.J. Abson and R.E. Dolby, *Welding Institute Research Report No. 19/1978*, Welding Institute, London, 1978.
10. M. Strangwood and H.K.D.H. Bhadeshia: in *Advances in Welding Science and Technology*, Proc. Conf., ASM INTERNATIONAL, Metals Park, OH, 1987, pp. 209-13.
11. M. Strangwood: Ph.D. Thesis, University of Cambridge, U.K., 1987.
12. J.-R. Yang: Ph.D. Thesis, University of Cambridge, U.K., 1987.
13. J.-R. Yang and H.K.D.H. Bhadeshia: in *Advances in Welding Science and Technology*, Proc. Conf., ASM INTERNATIONAL, Metals Park, OH, 1987, pp. 187-91.
14. H.K.D.H. Bhadeshia: *Phase Transformations 1987*, Proc. Conf., Institute of Metals, London, 1987, in press.
15. H.K.D.H. Bhadeshia and J.W. Christian: *Proc. Int. Conf. on Bainite*, Chicago, 1988, ASM, Metals Park, OH, in press.
16. J.W. Christian and D.V. Edmonds: *Phase Transformations in Ferrous Alloys*, Proc. Conf., A.R. Marder and J.I. Goldstein, eds., TMS-AIME, Warrendale, PA, 1984, pp. 293-325.
17. J.-R. Yang and H.K.D.H. Bhadeshia: *Welding Metallurgy of Structural Steels*, Proc. Conf., J.Y. Koo, ed., TMS-AIME, Warrendale, PA, 1987, pp. 549-56.
18. R.A. Ricks, P.R. Howell, and G.S. Barritte: *J. Mater. Sci.*, 1982, vol. 17, pp. 732-40.
19. R.F. Hehemann: *Phase Transformations*, ASM, Metals Park, OH, 1970, pp. 397-432.
20. H.K.D.H. Bhadeshia and D.V. Edmonds: *Acta Metall.*, 1980, vol. 28, pp. 1265-73.
21. R. Trivedi and G.M. Pound: *J. Appl. Phys.*, 1967, vol. 38, pp. 3569-76.
22. R.H. Siller and R.B. McLellan: TMS-AIME, 1969, vol. 245, pp. 697-700.
23. Richard H. Siller and Rex B. McLellan: *Metall. Trans.*, 1970, vol. 1, pp. 985-88.
24. H.K.D.H. Bhadeshia: *Met. Sci.*, 1981, vol. 15, pp. 477-79.
25. H.K.D.H. Bhadeshia, L.-E. Svensson, and B. Gretoft: *Acta Metall.*, 1985, vol. 33, pp. 1271-83.
26. H.K.D.H. Bhadeshia, L.-E. Svensson, and B. Gretoft: in *Advances in Welding Science and Technology*, Proc. Conf., ASM INTERNATIONAL, Metals Park, OH, 1987, pp. 225-29.
27. H.K.D.H. Bhadeshia: *Met. Sci.*, 1982, vol. 16 (3), pp. 159-65.
28. A.A.B. Sugden and H.K.D.H. Bhadeshia: *Metall. Trans. A*, 1988, vol. 19A, pp. 669-74.
29. H. Fredriksson: *Acta Universitatis Ouluensis*, University of Oulu, Oulu, Finland, 1983, Ser. 3, Tech. No. 26, pp. 1-24.
30. H. O'Neill: *Hardness Measurements of Metals and Alloys*, Chapman and Hall Ltd., London, 1967, pp. 43-44.